Defense Nuclear Agency
Alexandria, VA 22310-3398

DNA-TR-94-191

Equation of State Modeling for HYDROPLUS

Stephen Peyton
Maxwell Laboratories, Inc.
S-Cubed Division
P. O. Box 1620
La Jolla, CA 92038-1620

"Original contains color plates: All DTIC reproductions will be in black and white"

September 1995

Technical Report

CONTRACT No. DNA 001-93-C-0054

Approved for public release; distribution is unlimited.

Destroy this report when it is no longer needed. Do not return to sender.

PLEASE NOTIFY THE DEFENSE NUCLEAR AGENCY, ATTN: CSTI, 6801 TELEGRAPH ROAD, ALEXANDRIA, VA 22310-3398, IF YOUR ADDRESS IS INCORRECT, IF YOU WISH IT DELETED FROM THE DISTRIBUTION LIST, OR IF THE ADDRESSEE IS NO LONGER EMPLOYED BY YOUR ORGANIZATION.

DNA PRINTING PLANT

DISTRIBUTION LIST UPDATE

This mailer is provided to enable DNA to maintain current distribution lists for reports. (We would appreciate your providing the requested information.)

☐ Add the individual listed to your distribution list.

☐ Delete the cited organization/individual.

☐ Change of address.

NOTE:
Please return the mailing label from the document so that any additions, changes, corrections or deletions can be made easily. For distribution cancellation or more information call DNA/IMAS (703) 325-1036.

NAME: _____

ORGANIZATION: _____

OLD ADDRESS	CURRENT ADDRESS
_____	_____
_____	_____
_____	_____

TELEPHONE NUMBER: ( ) _____

DNA PUBLICATION NUMBER/TITLE	CHANGES/DELETIONS/ADDITIONS, etc.) *(Attach Sheet if more Space is Required)*
_____	_____
_____	_____
_____	_____

DNA OR OTHER GOVERNMENT CONTRACT NUMBER: _____

CERTIFICATION OF NEED-TO-KNOW BY GOVERNMENT SPONSOR (if other than DNA):

SPONSORING ORGANIZATION: _____

CONTRACTING OFFICER OR REPRESENTATIVE: _____

SIGNATURE: _____

CUT HERE AND RETURN

DEFENSE NUCLEAR AGENCY
ATTN: IMAS
6801 TELEGRAPH ROAD
ALEXANDRIA, VA 22310-3398

DEFENSE NUCLEAR AGENCY
ATTN: IMAS
6801 TELEGRAPH ROAD
ALEXANDRIA, VA 22310-3398

REPORT DOCUMENTATION PAGE

Form Approved
OMB No. 0704-0188

1. AGENCY USE ONLY (Leave blank)	2. REPORT DATE	3. REPORT TYPE AND DATES COVERED
	950901	Technical 930317 – 940817

4. TITLE AND SUBTITLE

Equation of State Modeling for HYDROPLUS

5. FUNDING NUMBERS

C - DNA 001-93-C-0054
PE - 62715H
PR - CD
TA - CD
WU- DH600190

6. AUTHOR(S)

Stephen Peyton

7. PERFORMING ORGANIZATION NAME(S) AND ADDRESS(ES)

Maxwell Laboratories, Inc.
S-Cubed Division
P.O. Box 1620
La Jolla, CA 92038-1620

8. PERFORMING ORGANIZATION REPORT NUMBER

SSS-DTR-94-14891

9. SPONSORING/MONITORING AGENCY NAME(S) AND ADDRESS(ES)

Defense Nuclear Agency
6801 Telegraph Road
Alexandria, VA 22310-3398
FCTTS/Rinehart

10. SPONSORING/MONITORING AGENCY REPORT NUMBER

DNA-TR-94-191

11. SUPPLEMENTARY NOTES

This work was sponsored by the Defense Nuclear Agency under RDT&E RMC Code T4613D CD CD 60019 5900A 25904D.

12a. DISTRIBUTION/AVAILABILITY STATEMENT

Approved for public release; distribution is unlimited.

12b. DISTRIBUTION CODE

13. ABSTRACT (*Maximum 200 words*)

This report reviews the theoretical foundation for the non-equilibrium equation of state for silicate rocks, and documents the parametric computational equation so state developed by S-Cubed for the DNA HYDROPLUS methodology. Model results for BEXAR rhyolite are presented.

14. SUBJECT TERMS

Computational	BEXAR	HYDROPLUS
Non-Equilibrium	Rhyolite	Yield Estimation
Equation of State	Phase Transition	Geologic Materials

15. NUMBER OF PAGES
28

16. PRICE CODE

17. SECURITY CLASSIFICATION OF REPORT	18. SECURITY CLASSIFICATION OF THIS PAGE	19. SECURITY CLASSIFICATION OF ABSTRACT	20. LIMITATION OF ABSTRACT
UNCLASSIFIED	UNCLASSIFIED	UNCLASSIFIED	SAR

NSN 7540-280-5500

Standard Form 298 (Rev.2-89)
Prescribed by ANSI Sts. 239-18
298-102

CLASSIFIED BY:

N/A since Unclassified.

DECLASSIFY ON:

N/A since Unclassified.

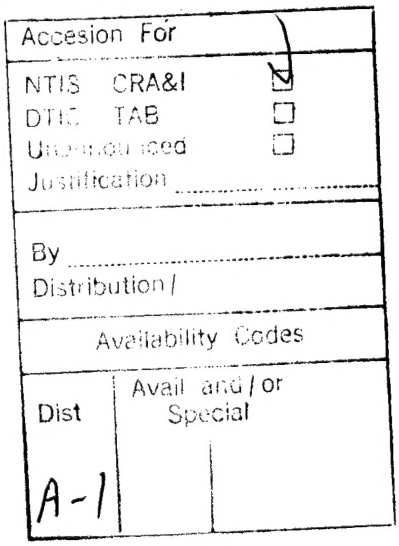

CONVERSION TABLE

Conversion factors for U.S. Customary to metric (SI) units of measurement

MULTIPLY →	BY →	TO GET
TO GET ←	BY ←	DIVIDE
angstrom	1.000 000 X E -10	meters (m)
atmosphere (normal)	1.013 25 X E +2	kilo pascal (kPa)
bar	1.000 000 X E +2	kilo pascal (kPa)
barn	1.000 000 X E -28	meter ^{2} (m^2)
British thermal unit (thermochemical)	1.054 350 X E +3	joule (J)
calorie (thermochemical)	4.184 000	joule (J)
cal (thermochemical)/cm^2	4.184 000 X E -2	mega joule/m^2 (MJ/m^2)
curie	3.700 000 X E +1	* giga becquerel (GBq)
degree (angle)	1.745 329 X E -2	radian (rad)
degree Fahrenheit	$t_K = (t^\circ f + 459.67)/1.8$	degree kelvin (K)
electron volt	1.602 19 X E -19	joule (J)
erg	1.000 000 X E -7	joule (J)
erg/second	1.000 000 X E -7	watt (W)
foot	3.048 000 X E -1	meter (m)
foot-pound-force	1.355 818	joule (J)
gallon (U.S. liquid)	3.785 412 X E -3	meter ^{3} (m^3)
inch	2.540 000 X E -2	meter (m)
jerk	1.000 000 X E +9	joule (J)
joule/kilogram (J/kg) (radiation dose absorbed)	1.000 000	Gray (Gy)
kilotons	4.183	terajoules
kip (1000 lbf)	4.448 222 X E +3	newton (N)
kip/inch ^{2} (ksi)	6.894 757 X E +3	kilo pascal (kPa)
ktap	1.000 000 X E +2	newton-second/m^2 ($N\text{-}s/m^2$)
micron	1.000 000 X E -6	meter (m)
mil	2.540 000 X E -5	meter (m)
mile (international)	1.609 344 X E +3	meter (m)
ounce	2.834 952 X E -2	kilogram (kg)
pound-force (lbs avoirdupois)	4.448 222	newton (N)
pound-force inch	1.129 848 X E -1	newton-meter (N•m)
pound-force/inch	1.751 268 X E +2	newton/meter (N/m)
pound-force/foot ^{2}	4.788 026 X E -2	kilo pascal (kPa)
pound-force/inch ^{2} (psi)	6.894 757	kilo pascal (kPa)
pound-mass (lbm avoirdupois)	4.535 924 X E -1	kilogram (kg)
pound-mass-foot ^{2} (moment of intertia)	4.214 011 X E -2	kilogram-meter ^{2} ($kg\cdot m^2$)
pound-mass/foot ^{3}	1.601 846 X E +1	kilogram/meter ^{3} (kg/m^3)
rad (radiation dose absorbed)	1.000 000 X E -2	** Gray (Gy)
roentgen	2.579 760 X E -4	coulomb/kilogram (C/kg)
shake	1.000 000 X E -8	second (s)
slug	1.459 390 X E +1	kilogram (kg)
torr (mm HG, O°C)	1.333 22 X E -1	kilo pascal (kPa)

* The becquerel (Bq) is the SI unit of radioactivity; 1 Bq = 1 event/s.
** The Gray (GY) is the SI unit of absorbed radiation.

A more complete listing of conversions may be found in "Metric Practice Guide E 380-74," American Society for Testing and Materials.

TABLE OF CONTENTS

FIGURES

SECTION 1
INTRODUCTION

The Protocol to the Threshold Test Ban Treaty (TTBT) provides for verification of a 150 kt limit on the yield of underground nuclear tests (UGT). The Protocol provisions for on-site inspection (OSI) include yield estimation by active close-in measurements during an UGT. The Defense Nuclear Agency (DNA) has the responsibility for yield estimation on a class of tests defined as 'non-standard' in the Protocol, and has developed a method called 'HYDROPLUS' for analyzing these tests. HYDROPLUS provides a yield estimate by comparing measured values of the shock stress, particle velocity, and time-of-arrival (or shock velocity) in the geologic medium surrounding the test region with theoretical predictions of these quantities.

In the HYDROPLUS methodology, the theoretical predictions are based on first-principles calculations of the evolution of the explosion-produced shock wave in the surrounding medium. Accurate predictions require the use of an appropriate computer code to solve the equations of motion, an adequate idealization of the test configuration, and accurate material models for the geological media and other materials surrounding the source.

For Treaty verification, yield uncertainties better than 30% with high confidence are required. This means that the combined error due to measurements and predictions must not exceed 30%. This places stringent requirements on the accuracy of both the measurements and the predictions.

The development of accurate equations of state (EOS) for geologic materials has emerged as a critical accomplishment for the success of HYDROPLUS. Early tests of the methodology revealed that conventional equilibrium equations of state were not capable of accurate predictions of the stress, particle velocity, and shock velocity simultaneously. Consistent predictions of all three shock features was shown to require non-equilibrium modeling of the phase transformation between low pressure and high pressure rock phases.

The application of HYDROPLUS also required the development of accurate site-specific equations of state on a short time line consistent with Protocol requirements.

S-Cubed has developed a parametric computational equation of state that accurately represents the observed non-equilibrium behavior. This equation of state has been implemented as part of a computer workstation encapsulation called HYPAWS, for *HYDROPLUS Analysis Workstation*. This program provides a convenient interactive capability for comparing the theoretical equation of state with laboratory test data, and varying model parameters to achieve the best agreement between the theoretical model and the data.

This report reviews the theoretical foundation for the non-equilibrium equation of state for silicate rocks, and documents the parametric computational equation of state developed by S-Cubed for the DNA HYDROPLUS methodology. Section 2 presents a qualitative discussion of the requirement for non-equilibrium equations-of-state, and the role of theoretical modeling in the formulation of the computational equation of state. Section 3 presents a qualitative discussion of the non-equilibrium model, while section 4 provides the mathematical details of the model. Section 5 presents additional details on the code implementation of the model and illustrates the results with an application to rhyolite. Conclusions and recommendations are presented in Section 6.

SECTION 2
EOS MODELING BACKGROUND

2.1 NEED FOR A NON-EQUILIBRIUM EQUATION OF STATE.

For some time, laboratory shock wave data have shown that granite and rhyolite display release paths that fall below the Hugoniot on a P-V plot. Such release paths are known to be inconsistent with equilibrium thermodynamic behavior.

Release paths have a direct influence on shock wave attenuation, and shock wave measurements on early tests of the HYDROPLUS method confirmed that releases beneath the Hugoniot occurred in full scale tests as well as laboratory scale tests. Consistent with this, it was demonstrated that equilibrium equations of state were not able to reproduce all the shock wave data.

The observed non-equilibrium behavior has a natural physical explanation associated with the non-equilibrium composition of polymorphic (distinct solid) phases of silica. This non-equilibrium phase phenomenon is characterized as phase hysteresis and profoundly affects ground shock propagation. The presence of phase hysteresis in large scale explosions has only become appreciated in the last few years. Previously, the best computational EOS models assumed phase equilibrium [Andrews, 1971; Lee et al., 1984].

The inadequacy of equilibrium EOS models emerged during the Defense Nuclear Agency's HYDROPLUS program. The HYDROPLUS requirement to make accurate predictions of particle velocity and shock pressure in addition to time-of-arrival made unprecedented requirements on the accuracy of computational models. The failure of conventional models to accurately predict all measured shock properties was apparent to all participants in this program. Schuster [1993], using empirical models, was the first to note that hysteretic models that agreed with laboratory data also produced ground shock predictions which agreed well with HYDROPLUS data. This demonstrated that hysteretic unloads were not just an artifact of laboratory experiments, but were essential to get detailed agreement with ground shock data.

The first ground shock calculations based on a thermodynamic model of non-equilibrium phase transitions were reported by Swegle [1990]. This paper contains a useful review of the evidence for non-equilibrium shock behavior of silica, the formulation of a theoretically sound computational model, and calculations which demonstrate the sensitivity of time-of-arrival to model details. Similar non-equilibrium models were developed independently by S-Cubed [Baker et al., 1993] and other DNA HYDROPLUS calculators.

2.2 THEORETICAL EQUATIONS-OF-STATE.

While purely empirical (based on data fitting with no theoretical constraints) EOS models have had significant successes in ground motion predictions, they can be used with confidence only for a limited range of conditions. Important physical processes such as melting, vaporization, chemical dissociation, and ionization cannot be accurately modeled by purely empirical methods. These processes must be realistically treated in the EOS for proper behavior at high temperatures and pressures. Because of this, computational equations of state (EOS subroutines) should have a good theoretical foundation.

Theoretical EOS models of the various physical processes have been implemented independently by a number of agencies. The documentation of the PANDA II code [Kerley, 1991] probably provides the best overview of these methods. The thermal component of the HYPAWS EOS is based on analogous models developed at S-Cubed.

The most significant element of the HYPAWS equation of state, however, is the effect of non-equilibrium solid-solid polymorphic phase transitions. Again, theoretical considerations provide improved confidence over purely empirical methods. In particular, thermodynamics is used to assure physically acceptable behavior. An important consequence of the thermodynamic models is that the hysteretic unloading behavior observed in laboratory experiments follow naturally from the second law of thermodynamics, *without curve fitting*.

The HYPAWS EOS integrates a non-equilibrium thermodynamic model of polymorphic phase transitions and an (equilibrium) thermal model of high temperature processes in a consistent manner. However, in contrast to the high temperature thermal model, the non-equilibrium phase model needs empirical data to calibrate its model parameters. It bears emphasis that the resulting model satisfies the general theoretical requirements of thermodynamics, whereas a purely empirical model will not.

This semi-empirical approach is necessary for a number of reasons. The most fundamental reason is that accurate *ab initio* predictions of the response of complicated geologic materials in the regime of interest is not now scientifically feasible. If it were, laboratory shock wave data would not be as important as it now is. A major reason for this is that the mechanism for non-equilibrium behavior is not well understood. Furthermore, if the theoretical capability did exist, the detailed microscopic structure for the subject rock will not be available. Finally, time constraints for HYDROPLUS analysis preclude detailed theoretical analysis.

The hysteretic model, like other aspects of the equation of state is a mixture of theory (thermodynamics) and experimental calibration (using shock wave data). The shock wave data is interpreted in the context of a two phase model using parametric models of the low pressure phase (LPP), the high pressure phase (HPP)

and the mixed phase Hugoniots. The hysteretic behavior is then partially derived from thermodynamic laws, and partially fitted to test data. In particular, the second law of thermodynamics dictates that the fraction in the high pressure phase cannot decrease for pressures above the LPP-HPP boundary, so the fraction in the high pressure phase is initially frozen (held fixed). This procedure generally gives remarkably good agreement with the observed release data. At lower pressures recovery of the low pressure phase is possible, and the model release curves are adjusted to agree with observations. This fitting procedure is facilitated by the HYPAWS EOS module. These issues will be discussed in more detail in succeeding sections.

SECTION 3
NON-EQUILIBRIUM CONSIDERATIONS

Phase hysteresis can be explained with a simple physical model. The material in question begins in a low pressure phase which is stable at pressures below some transition pressure (P_{start}). When the shock strength exceeds the transition pressure, the low pressure phase is no longer stable, but the transformation to a high pressure phase is inhibited by slow transformation kinetics. The non-equilibrium low pressure phase deforms inhomogeneously and partially transforms to a high pressure phase in localized regions. The extent of transformation from the low pressure to high pressure phases increases as the shock pressure increases. The Hugoniot state in this transition region is not in thermodynamic equilibrium because of the non-equilibrium phase composition.

Consider an adiabatic release path from a non-equilibrium Hugoniot state. Non-equilibrium thermodynamics constrains what can happen on this path. As long as conditions remain outside the stability domain of the low pressure phase, no reverse transformation from a high pressure phase to the low pressure phase can occur. This is a profound and inescapable consequence of non-equilibrium thermodynamics, and leads directly to the observed anomalous releases below the Hugoniot in the transition region.

The behavior discussed above is appropriately called phase hysteresis. The inability to revert to the low pressure, low density phase upon unloading has a significant effect on wave propagation. The principal effect of phase hysteresis is increased attenuation of the shock wave. This is because the energy required to transform from the low pressure phase to the high pressure phase cannot be recovered until the low pressure phase is again stable. This is analogous to simple models of pore collapse where the energy involved in collapsing pores is never recovered.

The practical consequence of using a hysteretic phase transformation model is that one can easily calibrate the model to laboratory shock wave data, and then accurately reproduce pressures, particle velocities, and times of arrival for well instrumented underground nuclear tests. Conventional (*i.e.*, non-hysteretic) equation of state models have failed to achieve this level of agreement for pressure, particle velocity, and time-of-arrival simultaneously.

A non-equilibrium equation of state entails modeling issues that are not present for a conventional equation of state. In general, the independent variables, matter density, specific internal energy (or temperature), and composition must be specified in order to determine the pressure. By 'composition', we mean the fractions of the low and high pressure phases. For thermodynamic equilibrium, the composition is uniquely determined (from thermodynamic theory) as a function of the matter density and specific internal energy. For a non-equilibrium system, an

independent criterion for determining the composition must be provided. Theory provides very general constraints on the composition, but very little guidance on details. This permits appropriate empirical methods to satisfy general theoretical constraints.

The detailed modeling of the non-equilibrium composition is basically empirical. It should be noted that this is not essentially different than other types of equation of state or constitutive modeling. There is generally no theoretical basis for choosing a particular functional form for any constitutive characteristic. It is up to the modeler to discover functional forms which satisfy theoretical constraints and are consistent with observed behavior. Likewise, the parameters of the model are chosen to agree with observations. The principal challenge to such models is that they should continue to agree with observations in new physical regimes.

SECTION 4
DISCUSSION OF MODEL

A computational non-equilibrium equation of state which accounts for the key features of a non-equilibrium silicate phase transformation has been implemented in HYPAWS. This equation of state is based on a physical model of the phase transformation using the thermodynamic mixture theory [Gibbs, 1948]. The model assumes that the material can exist in two distinct phases, a low pressure phase (LPP) which is stable at low pressures, and a high pressure phase (HPP) which is stable at high pressures. At intermediate pressures, the two phases are assumed to occur with non-equilibrium concentrations.

The HYPAWS equation of state method combines analytic and tabular components. The analytic part consists of parametric representations of reference adiabats of the LPP and HPP constituents, and a model of the mixed phase regime. The reference adiabats represent static loading from standard reference states for the low pressure and high pressure phases (room temperature and zero pressure). The tabular part consists of a full thermodynamic equation of state which provides the thermal pressure as a function of the matter density and thermal energy. The pressure is determined as the sum of the analytic and tabular components. This is discussed in more detail below.

4.1 THE TABULAR COMPONENT.

The tabular component of the EOS consists of a full thermodynamic equation of state for silicate rocks developed at S-Cubed. The tabular model reflects the physics of melting, vaporization, chemical dissociation, and ionization and accounts for the dependence of both pressure and temperature on the material density and specific internal energy. Due to the complexity of the tabular component, it is not adjustable within HYPAWS. It is also worth noting that the tabular EOS is not just a computational convenience, but is required because the theoretical basis of the equation of state does not lead to an analytic form. The following discussion provides a brief summary of the theoretical basis for the tabular component of the equation of state.

The EOS is derived from a Helmholtz potential [Callen, 1985], which guarantees thermodynamic consistency. The Helmholtz potential (or Helmholtz free energy) depends explicitly on the temperature (ϑ), the density (ρ) and the system composition $\{N_i\}$

$$F = F(\vartheta, \rho, \{N_i\})$$

and consists of a sum of terms that account for various physical components of the free energy. These terms are described in detail by Kerley.

The formulation of the Helmholtz potential is only a first step in constructing a computational equation of state. At high temperatures where chemical dissociation or ionization occur, the composition of the system is not fixed. If thermodynamic equilibrium is assumed, the composition, $\{N_i\}$, is determined by minimizing the free energy (equivalent to maximizing the entropy). Thus, the composition is fixed by the temperature and density and is no longer an explicit independent variable. (In the non-equilibrium mixed phase regime, the phase composition must be determined independently.)

The Helmholtz potential can be decomposed into a cold contribution (F_C) and a thermal contribution (F_T)

$$F = F_C(\rho) + F_T(\vartheta, \rho)$$

The separation of the computational equation of state into an analytic term that is independent of temperature, and a tabular thermal term is related to this decomposition.

Given the Helmholtz potential, thermodynamic properties of computational interest can be explicitly derived, *e.g.*, the pressure (P) and specific internal energy (ε) are given by

$$P = \rho^2 \frac{\partial F}{\partial \rho}$$

and

$$\varepsilon = F - \vartheta \frac{\partial F}{\partial \vartheta}$$

Because ρ and ε are the natural independent variables for hydrodynamic computations, these equations must be numerically inverted to provide ϑ and P as a function of ρ and ε. This presents a choice of iterating within the calculation or using tables, and is one reason for using tabular equations of state. There are other reasons which are addressed below.

The Helmholtz free energy applies to a single phase, so the solid, liquid and vapor phases each have distinct Helmholtz potentials. The equation of state must uniquely account for the phase composition. With the exception of the solid-solid polymorphic phase transitions this is accomplished with the classical thermodynamic treatment of phase equilibria. This requires using the Gibbs potential:

$$G = F + \frac{P}{\rho}$$

The Gibbs potential depends explictly on the pressure and temperature. In general, phase equilibrium is achieved by selecting the phase with the minimum

Gibbs energy. Regions (in P, ϑ space) in which a particular phase is stable are separated by lines (coexistence lines) for which the Gibbs energies in the neighboring phases are equal. On the coexistence line, the matter density and the specific internal energy can vary continuously between those of the bounding phases. The phase boundaries must be determined numerically with a Gibbs/Maxwell construction [Callen, 1985]. This is another reason for using tabular equations of state.

The full equation of state must account for a number of distinct physical phenomena including: polymorphic phase transitions, melting, vaporization, dissociation, and ionization. Specialized first-principles codes exist for some of these phenomena while others require a more empirical approach. The complexity of phenomena and the need to cover a wide range of temperatures and pressures dictate that the best physically based equation of state models are tabular in nature. Due to the technically complicated nature of the high temperature equation of state, it was not feasible to include the capability to adjust the thermal model in HYPAWS. This is, however, a potential area for improving the HYPAWS treatment.

Shock propagation in the HYDROPLUS regime is most sensitive to the pressure response at relatively low temperatures. Therefore, it was decided to separate the full equation of state into a 'cold' component and a thermal component. The cold component is analytic and can be adjusted by fitting to shock wave data while the thermal component consists of a fixed table derived from detailed high temperature theories. The cold and thermal components are integrated into a consistent model, and are never applied in isolation. It is not appropriate to think in terms of a 'thermal correction'. The combined equation of state depends on the usual independent variables, matter density, specific internal energy, and in our case on the hysteretic parameter, f. In addition, it also depends on the parameters of the analytic model. These parameters are adjusted so that the equation of state agrees with the shock wave experiments. This parameter fitting is easily accomplished within HYPAWS using the EOS module. Once the parameters are set, the combined equation of state is used directly in the finite difference solution.

4.2 THE ANALYTIC COMPONENT.

The analytic part consists of parametric representations of adiabatic loading for the LPP and HPP using the Murnaghan equation of state, and a parametric representation of the non-equilibrium mixed phase region. Three parameters are required for each pure phase, and four parameters for the transition region, for a total of 10 parameters. These parameters can be set in the HYPAWS user interface to obtain the best agreement between the computational equation of state and laboratory EOS data. The three parameters for the HPP and LPP are ρ_0, K_0, and K'_0 in the Murnaghan equation of state:

$$P_0 = \frac{K_0}{K_0'}\left(\left(\frac{\rho}{\rho_0}\right)^{K_0'} - 1\right)$$

where ρ_0 is a reference density (zero pressure) for the phase under consideration, K_0 is a reference bulk modulus (zero pressure), and K'_0 is the 'slope' (called 'n' in the HYPAWS interface). From the definition of the bulk modulus

$$K = \rho\frac{\partial P}{\partial \rho}$$

the Murnaghan equation gives,

$$K = K_0 + K_0' P$$

so

$$K_0' = \frac{\partial K}{\partial P}$$

is the slope of the bulk modulus as a function of pressure.

Generally, for rock K'_0 is in the range 3 to 6 and K_0 is hundreds or thousands of kbar. The LPP and HPP phases are independently fit to the full equation of state to determine the Murnaghan parameters.

The parameters of the Murnaghan equation are internal to the equation of state module, and are determined automatically when the full equation of state is fitted to shock wave data using the HYPAWS EOS module.

4.3 THE MIXED PHASE REGIME.

The solid-solid polymorphic phase transition is treated with an analytic non-equilibrium model. The need for the non-equilibrium model is illustrated by considering the laboratory Hugoniot (shock) and release data for quartz monzonite obtained by Ahrens [personal communication] . Hugoniot data are shown as points, and release data as connected points in Figure 4-1. This Figure emphasizes the 100 to 500 kbar range, where the silica high pressure phase is stable. The four lower pressure release adiabats make a compelling case for non-equilibrium mixed phase behavior.

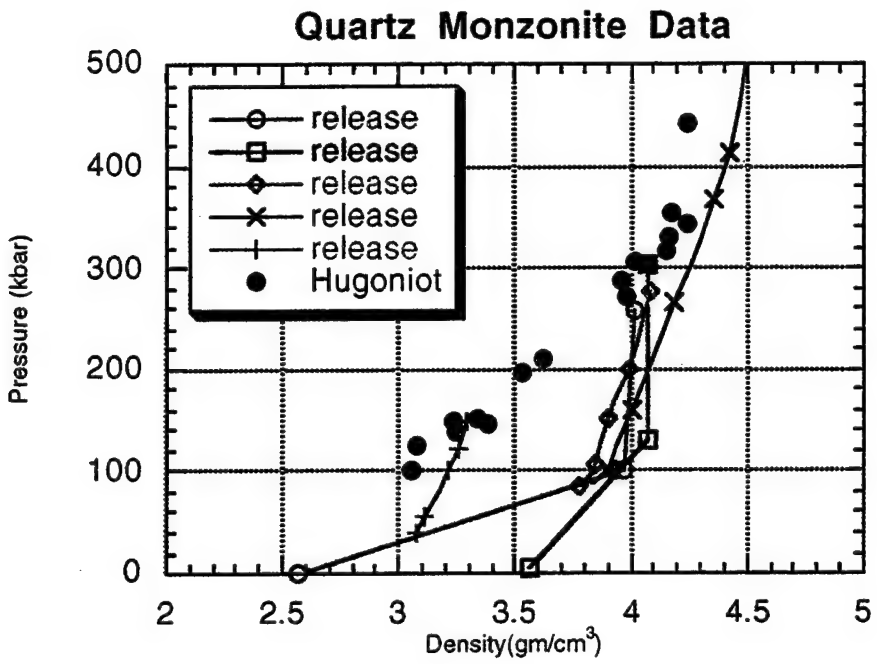

Figure 4-1. Experimental Hugoniot and release adiabats for quartz monzonite.

SECTION 5
RHYOLITE ANALYSIS

Figure 5-1 shows a plot for SNLA rhyolite analogous to Figure 4-1 that was available pretest for BEXAR. This data set is obviously sparse and problematic. In particular, there was little data above the quartz - stishovite phase boundary. Consequently, the equation of state developed for the BEXAR HYDROPLUS exercise had to be based on related EOS data and judgement. (In a real HYDROPLUS application, much more data is expected.)

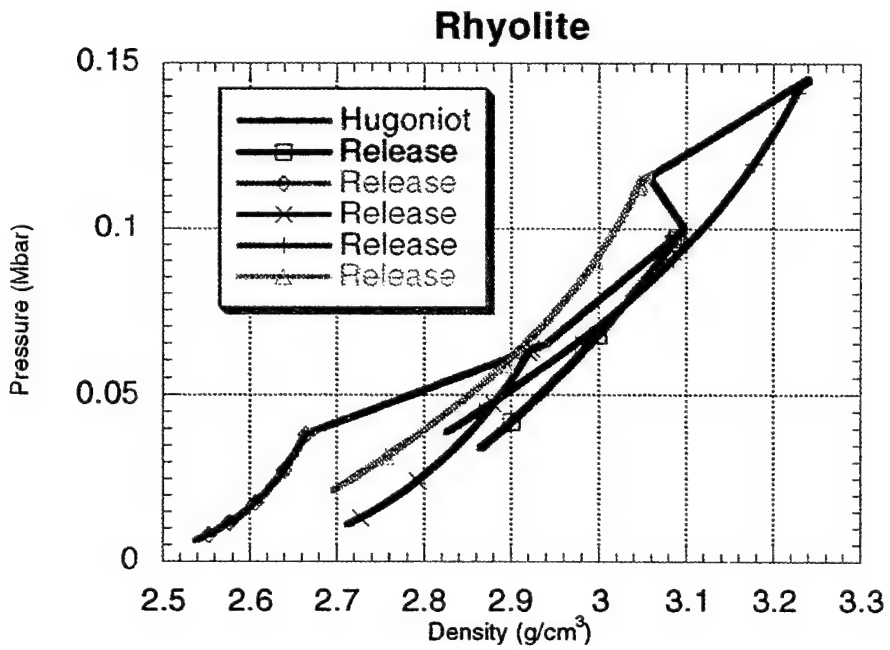

Figure 5-1. Experimental Hugoniot and release adiabats for BEXAR rhyolite.

The densities obtained on shock loading show that the silica is not completely converted to the high pressure phase until roughly 400-500 kbar. (The LPP and HPP for silica are quartz and stishovite, respectively.) Under static loading, this transformation would be complete at roughly 100 kbar. This is a clear demonstration that phase equilibrium is not established during shock loading. The releases beneath the Hugoniot are also a consequence of the non-equilbrium phase composition, and cannot be produced with an equilibrium equation of state.

To model the non-equilibrium phase transition, the phase composition is not determined within the equation of state, but by a model (described below) that determines the phase composition based on the hydrodynamic history of the material.

To deal with the non-equilibrium phase transition, we must explicitly introduce the non-equilibrium mass fractions of the low pressure phase (LPP), f_1 and the high pressure phase (HPP), f_2. The mass fractions satisfy the constraint (mass conservation)

$$\sum_i f_i = 1$$

It is also required that $0 \le f_i \le 1$. The mass fraction of the HPP is also represented by f - without a subscript, *i.e.*, $f=f_2=1-f_1$. f is an additional dynamical variable that must be tracked by the hydrocode.

The material is now modeled as a mixture of the LPP and HPP with an explicit dependence on mass fraction. The specific volume ($\tau=1/\rho$) satisfies

$$\tau = \sum_i f_i \tau_i$$

and the specific internal energy (ε)satisfies

$$\varepsilon = \sum_i f_i \varepsilon_i$$

where τ_i and ε_i are the specific volume and specific internal energy of each phase i. In the Gibbs representation, τ_i and ε_i are functions of P and ϑ, so τ and ε are functions of P, ϑ and f. Note that this is an implicit functional dependence because P and ϑ are functions of τ_i and ε_i. It follows that P and ϑ are functions of τ, ε , and f. This is an implicit functional dependence.

Once the LPP and HPP regimes have been fit, the mixed phase regime is treated independently with four additional parameters. Two of these parameters P_{start} and P_{end}, identify the pressures at which the phase transition begins and ends (the intersections of the pure and mixed phase regimes on the Hugoniot) and two parameters, n_{load} and n_{unload}, determine the shape of the loading and unloading curves.

P_{start}, P_{end} and n_{load} explicitly control the shape of the model Hugoniot in the mixed phase regime. These parameters are adjusted so that the model is consistent with data points that are identified as mixed phase points. This is illustrated in Figure 5-2 with a plot of shock velocity vs. particle velocity, where the mixed phase region extends roughly from 1 to 2 km/s on the abscissa. All available rhyolite data have been included in this plot, and were considered in developing the model. The data scatter in the low velocity region illustrates the need for site-specific data. The fit in this regime was not well constrained by the data, and was based largely on scientific judgement.

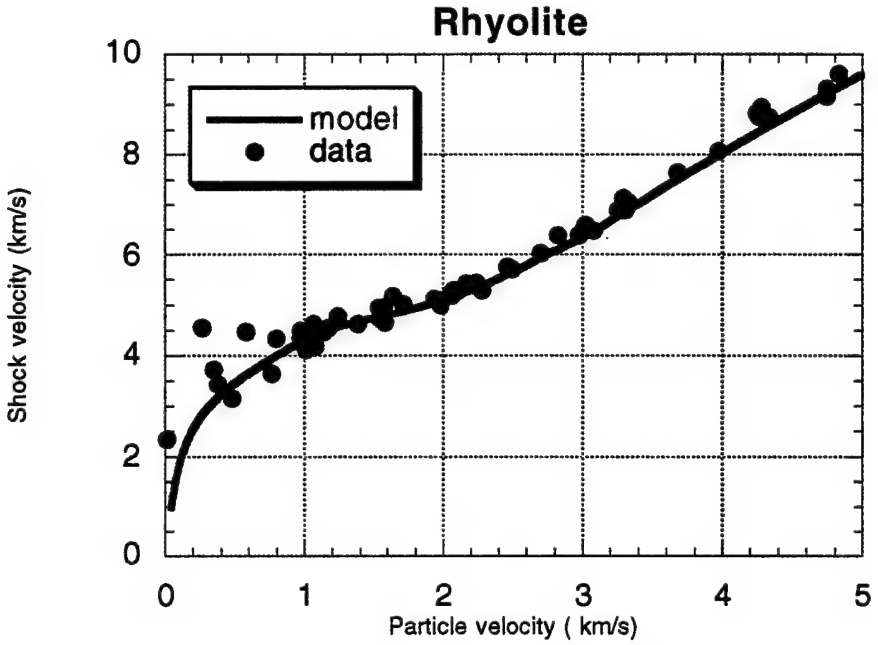

Figure 5-2. Shock velocity vs. particle velocity for rhyolite.

The incorporation of these parameters into the computational equation of state is transparent to the user, but some further details will be discussed for completeness. The four mixed phase parameters are used in the non-equilibrium model for the concentration of the HPP, f. The model for f is constrained by the second law of thermodynamics, which requires non-negative changes in the entropy as a function of time. Therefore, f cannot decrease unless $P<P_{start}$, increase unless $P>P_{start}$. This fundamental requirement is responsible for the observed phase hysteresis.

The behavior on loading is thus given by

$$f_{load} = 0 \text{ for } P \le P_{start}$$

$$f_{load}(\tau) = \left(\frac{\tau_{start} - \tau}{\tau_{start} - \tau_{end}} \right)^{n_{load}} \text{ for } P_{start} < P < P_{end}, \text{ and}$$

$$f_{load} = 1 \text{ for } P_{end} \le P$$

where τ_{start} and τ_{end} are the specific volumes at P_{start} and P_{end}, and are computed in the code from the respective fits to the LPP and HPP Hugoniot data. Fitting the mixed phase Hugoniot is, therefore, equivalent to estimating the phase composition

on loading as a function of specific volume. On loading, f=0 or 1 depending on whether $P \leq P_{start}$ or $P_{end} \leq P$ (*i.e.*, pure LPP or HPP).

On unloading, f cannot decrease unless $P \leq P_{start}$. If we assume that we have converted completely to the HPP, we can define

$$f_{unload}(\tau) = \left(\frac{\tau_{lpp}(0) - \tau}{\tau_{lpp}(0) - \tau_{hpp}(P_{start})} \right)^{n_{unload}}$$

so that f=1 when τ equals the specific volume of the HPP at P_{start}, and f=0 at the normal specific volume of the low density phase. This expression assumes that complete conversion does not occur without a significant volume recovery. The parameter n_{unload} controls the shape of this function.

Hysteresis, or memory, is handled computationally by carrying the composition, f, as an independent variable which can reflect the material history. The values of f_{load} and f_{unload} are provisional values of f that are determined by the current state alone. During loading, $f<f_{load}$, and f is updated so $f=f_{load}$, *i.e.*, the fraction in the high pressure phase is increased. During unloading $f>f_{load}$, and the composition remains frozen so long as $f<f_{unload}$. Finally, if $f>f_{unload}$, f is updated so that $f=f_{unload}$, *i.e.*, the fraction in the high pressure phase is reduced. This occurs in the stability domain of the LPP, where the reverse transformation can occur. The computer algorithm for this is

```
f=MIN(MAX(f,fload),funload)
```

Thus, all unloads in the mixed phase regime initially have a frozen phase composition and then follow a universal recovery curve. There is no independent control of the unloads in the frozen phase regime. In the final portion of the unload, phase recovery is controlled by the single parameter, n_{unload}. Note that it is possible to produce *unphysical* results with a poor choice of this parameter. It is also noteworthy that this portion of the unloading path is not well constrained by data. The value $n_{unload}=1.25$ generally gives acceptable results. It is fortunate that uncertainties in this regime are not generally important for ground shock predictions.

Figure 5-3 illustrates the general behavior of the EOS model for rhyolite. The agreement between the model and data is illustrated in Figure 5-4. The monzonite model and data are compared here because of the availability of data releases for monzonite in the mixed phase regime.

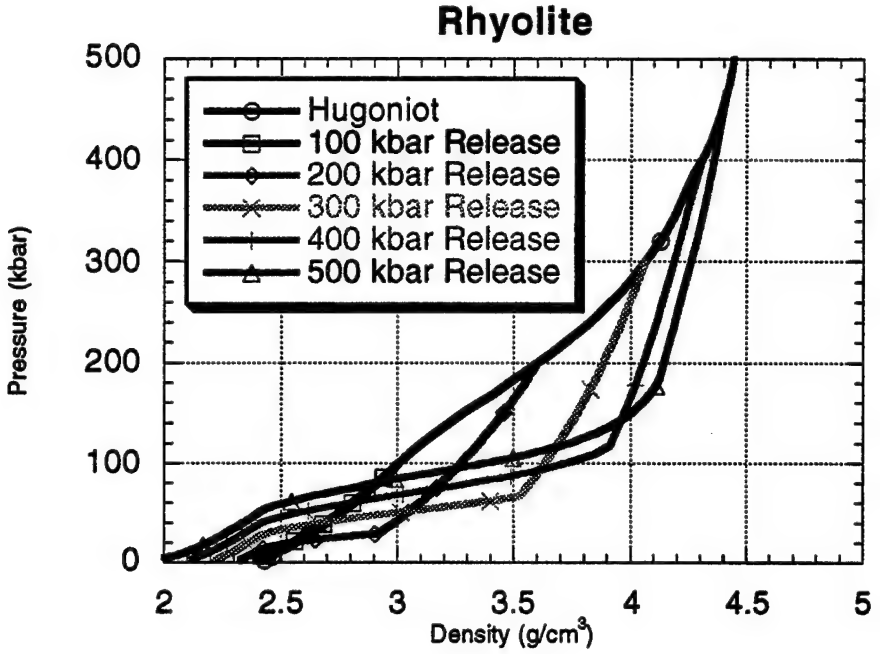

Figure 5-3. Pressure vs. density for the rhyolite EOS model.

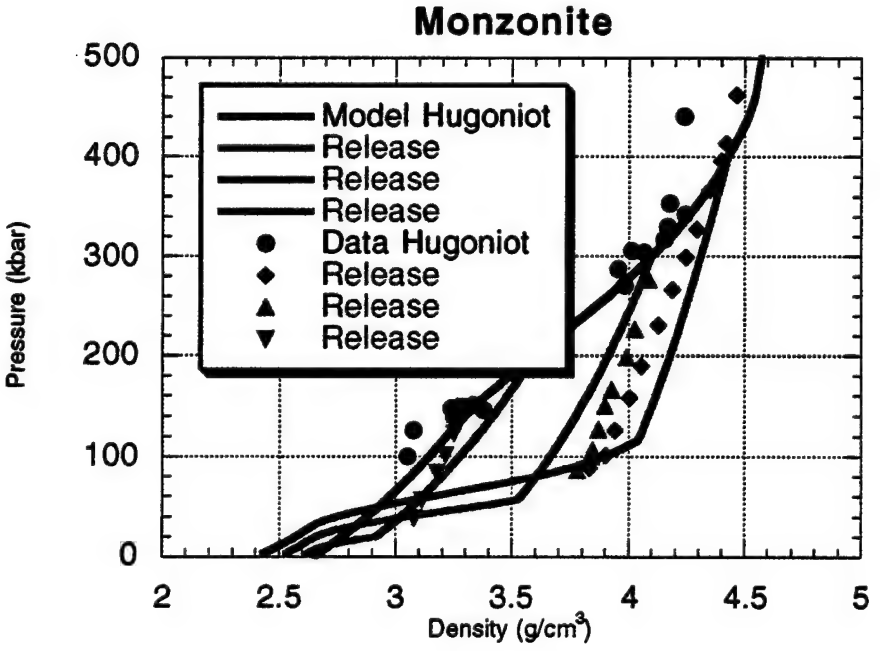

Figure 5-4. Comparison of model EOS and data. The comparison here is for Monzonite.

The parameters for the rhyolite fit are:

	Pure Phase Parameters	
	LPP	HPP
ρ_0	2.41078470 g/cm^3	4.0 g/cm^3
K_0	270 kbar	3.0 Mbar
n	4.0	5.0

	Mixed Phase Parameters
P_{start}	100 kbar
P_{end}	400 kbar
n_{load}	1.6
n_{unload}	1.25

Note that the large bulk moduli lead to large variations in pressure for small variations in the density making precision of the reference density very important. This explains the high precision of the reference density for the LPP.

We want to emphasize that the hysteretic unload is influenced by a single parameter, n_{unload}, while all other parameters associated with the mixed phase region are obtained from the Hugoniot response. Furthermore, n_{unload} has no effect on initial unloading from the Hugoniot state, but is only important at pressures below P_{start}. ***It follows that this unloading parameter has almost no effect on shock evolution and yield estimation.*** The essential characteristics of the hysteretic unload are not modeled independently, but are physical consequences of the theory of non-equilibrium phase transitions and the parametric represention of the phase transition *on the Hugoniot*. The EOS prediction for initial release behavior near the Hugoniot thus represents an independent prediction of the model, and is not obtained by fitting release behavior. The comparison between the model releases and release data obtained is a critical test of the model, and the striking agreement for monzonite provides strong support for this modeling approach.

SECTION 6
CONCLUSIONS AND RECOMMENDATIONS

The development of a practical methodology for treaty verification has necessitated an improved quantitative treatment of the dynamic high pressure behavior of geologic materials. Non-equilibrium phase transformations in geologic material have moved from curiosity and conjecture to clear fact, and theoretically sound models have been developed to describe this behavior. Nevertheless, our understanding of this behavior remains imperfect. The model presented here is believed to be adequate for the intended purpose inasmuch as it appears capable of reproducing shock loading and unloading data.

The model is nevertheless incorrect in detail. In particular, investigations have shown that the inhomogeneous shock loading results in heated shear bands in which the transformation to the dense phase occurs. The heating clearly accelerates the transformation to the dense phase, and also results in the production of a liquid phase. It is undoubtedly an oversimplification to regard the high pressure phase as pure stishovite. Furthermore, the possible role of material strength has not been fully explored.

In shelving HYDROPLUS, we are shelving an unfinished EOS research program. Improved models of the shock induced phase transformation may emerge while HYDROPLUS is on the shelf. Or, reduced support for science in general may result in little advancement in this area. Should the need for HYDROPLUS reemerge, there are interesting equation of state issues which should be reopened.

SECTION 7
REFERENCES

Andrews, D. J., "Calculation of Mixed Phases in Continuum Mechanics,"(U) J. Comp. Phys. 7, 310 (1971)) or Lee, et. al. (Lee, C. K. B., J. Baker, and S. Peyton, "The Effect of Equilibrium Modeling of Saturated Quartz in Energy Coupling Calculations, Shock Waves in Condensed Matter, 1983,"(U) J. R. Asay, R. A. Graham, G. K. Straub (editors) ©Elsevier Science Publishers B. V., 1984. (U)

Baker, J., Higginbotham, M., Patnaik, P., Peyton, S., "Distant Zenith Calculations and Near Source Choke Issues,"(U) Proceedings of the Defense Nuclear Agency Verification Technology – HYDROPLUS Ground Shock Measurement Technology and Yield Determination (VERITECH) Symposium, 2-4 February 1992, DASIAC TR-92-002-V1, 1993]. (U)

Callen,Herbert B., "Thermodynamics and an Introduction to Thermostatistics,"(U) John Wiley & Sons, Inc. (1985). (U)

Gibbs , J. Willard, The Collected Works, Yale University Press, Vol. I, 1948. (U)

Kerley, G. I., "User's Manual for PANDA II: A Computer Code for Calculating Equations of State,"(U) Sandia SAND 88-2291, 26 June 1991. (U)

Schuster, S., "Empirical EOS Models," (U) Proceedings of the Defense Nuclear Agency Verification Technology – HYDROPLUS Ground Shock Measurement Technology and Yield Determination (VERITECH) Symposium, 2-4 February 1992, DASIAC TR-92-002-V1, 1993. (U)

Swegle, J. W., "Irreversible phase transitions and wave propagation in silicate geologic materials,"(U) J. Appl. Phys., Vol. 66. No. 4, 15 August 1990. (U)

DISTRIBUTION LIST

DNA-TR-94-191

DEPARTMENT OF DEFENSE

DEFENSE INTELLIGENCE AGENCY
ATTN: DT-1

DEFENSE NUCLEAR AGENCY
ATTN: DFSP
ATTN: DFTD D LINGER
ATTN: SPWE
2 CY ATTN: SSTL
ATTN: TDTV F RENSVOLD

DEFENSE TECHNICAL INFORMATION CENTER
ATTN: DTIC/OC

FIELD COMMAND DEFENSE NUCLEAR AGENCY
ATTN: FCTN B HARRIS-WEST
ATTN: NVTV

FIELD COMMAND DEFENSE NUCLEAR AGENCY
ATTN: FCTO M OBRIEN
ATTN: FCTT-T E RINEHART
ATTN: FCTT DR BALADI
ATTN: FCTTS
ATTN: FCTTS A MARTINEZ
ATTN: FCTTS D SEEMANN
ATTN: FCTTS J LEVERETTE
ATTN: FCTTS LTCOL LEONARD
ATTN: FCTTS P RANDLES

DEPARTMENT OF THE ARMY

U S ARMY ENGR WATERWAYS EXPER STATION
ATTN: E JACKSON CEWES-SD-R
ATTN: J ZELASKO CEWES-SD-R

DEPARTMENT OF THE AIR FORCE

PHILLIPS LABORATORY
ATTN: PL/SUL

DEPARTMENT OF ENERGY

EG&G, INC
ATTN: D EILERS

LAWRENCE LIVERMORE NATIONAL LAB
ATTN: DONALD LARSON
ATTN: F HEUZE L-200
ATTN: L-13 B DUNLAP
ATTN: L-200 LEWIS GLENN
ATTN: L-200 J RAMBO
ATTN: L-200 J WHITE
ATTN: L-200 W C MOSS
ATTN: L-58 R WARD
ATTN: TECH LIBRARY

LOS ALAMOS NATIONAL LABORATORY
ATTN: DAVID KING
ATTN: FRED APP
ATTN: T KUNKLE
ATTN: T MCKOWN
ATTN: J FRITZ
ATTN: C MORRIS
2 CY ATTN: REPORT LIBRARY
ATTN: J N JOHNSON
ATTN: THOMAS DEY
ATTN: TOM WEAVER

SANDIA NATIONAL LABORATORIES
ATTN: DIV 9321 W BOYER
ATTN: MIKE FURNISH
2 CY ATTN: TECH LIB 3141

DEPARTMENT OF DEFENSE CONTRACTORS

DEFENSE GROUP, INC
ATTN: ROBERT POLL

ENSCO INC
ATTN: P FISHER

JAYCOR
ATTN: CYRUS P KNOWLES

KAMAN SCIENCES CORP
ATTN: DASIAC

KAMAN SCIENCES CORPORATION
2 CY ATTN: DASIAC

KTECH CORP
ATTN: E SMITH
ATTN: FRANK DAVIES
ATTN: L LEE

LOGICON R & D ASSOCIATES
ATTN: J RENICK
ATTN: L GERMAIN

MAXWELL LABORATORIES INC
ATTN: DR E PETERSON
ATTN: J BAKER
ATTN: J MORRIS
ATTN: MARK GROETHE
ATTN: P COLEMAN
2 CY ATTN: S PEYTON

SCIENCE APPLICATIONS INTL CORP
ATTN: DAN PATCH
ATTN: DR M MCKAY
ATTN: JACK KLUMP
ATTN: L SCOTT
ATTN: MARTIN FOGEL

SRI INTERNATIONAL
ATTN: DR JIM GRAN
ATTN: P DE CARLI

TECH REPS, INC
ATTN: F MCMULLAN
ATTN: R NAEGELI

TERRA TEK, INC
ATTN: W MARTIN

TITAN CORPORATION (THE)
ATTN: ANNE COOPER
ATTN: S SCHUSTER

DIRECTORY OF OTHER

MARYLAND UNIVERSITY OF
ATTN: RICHARD DICK